NOTICE CONCERNING COPYRIGHT RESTRICTIONS

Detection of a Reservoir Fracture by the Use of Sonic Log Data in EE-4, Higashi-Hachimantai

Hiroyuki Saito and Kazuo Hayashi

Institute of Fluid Science, Tohoku University
Sendai, 980-8577, Japan

ABSTRACT

This paper investigates the change of aperture of a fracture caused by borehole pumping with full-waveform acoustic logs (FWAL). The FWAL data was collected in the Higashi-Hachimantai Hot Dry Rock model field, Japan. In this field, a single fracture was induced hydraulically in intact welded tuff. The fracture aperture can be controlled by injection of water into the borehole. At the depth of the artificial fracture, P-wave and tube-wave amplitude deficits were observed. Time-frequency analysis was applied to obtain the rate of amplitude deficits in the frequency domain. Based on the depth range of the observed amplitude deficits, it is clear that there is a permeable zone about 1.4m wide around the fracture. The amplitude deficits increased when wellhead pressure was increased from 0MPa to 3MPa. The maximum P-wave amplitude deficit rose from 76% to 85% and that of the direct tube-wave rose from 12% to 16%. A parallel plate fracture model was examined to estimate the fracture aperture using the amplitude deficit of the direct tube-wave. Estimated fracture aperture increased from 2.5mm to 3.5mm as wellhead pressure increased.

Introduction

The aperture of a fracture that governs the amount of fluid conducted into the borehole is an important parameter when extracting geothermal energy. A variety of methods are employed to detect and to characterize open fractures. It has been recognized that full-waveform acoustic logging is one of the most useful methods to detect the open borehole fractures since on a borehole Stoneley wave has a large amount of energy at relatively low frequencies and is sensitive to open fractures.

Paillet (1980) discussed the effect of fractures intersecting the borehole on the logging waveforms. Since then, evaluation methods of fracture properties have been studied based on field data, theoretical modeling, and ultrasonic laboratory models. A model by Mathieu (1984) has been used to model Stoneley wave attenuation across a fracture. Hardin *et al.* (1987) examined the Mathieu model and found qualitative and rough quantitative correlation between the model and field data. Tang and Cheng (1989) studied the effect of fluid viscosity and dynamic fluid flow in a fracture. Hornby *et al.* (1989) calculated the transmission and reflection coefficients of Stoneley waves at a plane fracture by omitting the viscous effects. The two theories with the plane fracture (Tang and Cheng, 1989; Hornby *et al.*, 1989) are good agreement with the Laboratory data.

In the Higashi-Hachimantai Hot Dry Rock model field (Niitsuma, 1989), a single fracture was induced hydraulically; therefore we can carry out experiments varying the aperture as a parameter. The P-wave and S-wave travel time delays were observed in the cross-hole seismic measurement during pressurization of the fracture (Niitsuma and Saito, 1991a; Moriya and Niitsuma, 1995). Niitsuma and Saito (1991a) reported the existence of a low-velocity zone in the vicinity of the fracture.

In this paper, we examine the method of Tang and Cheng (1989) based on the FWAL data collected during borehole pumping and evaluate the reopening behavior of the fracture. In addition, we clarify the thickness of permeable zone in the vicinity of the fracture.

Study Site and Field Experiment

The Higashi-Hachimantai Hot Dry Rock model field for this study is located in Iwate Prefecture, Japan (Niitsuma, 1989). Figure 1 (overleaf) depicts the Higashi-Hachimantai field. A subsurface fracture was created at a depth of 369.0m in F-1 well by hydraulic fracturing. The bedrock in which the artificial fracture was created is an intact welded tuff, which has no significant joints or fractures. Well EE-4 was drilled into the fracture after fracturing, and intersected at a depth of 358.2m. The strike and dip of the fracture are N61°E and N46°W, respectively. Niitsuma and Saito (1991b) estimated the 3-D configuration of fracture by the triaxial shear-shadow method and showed that the fracture was about 60m in diameter. The relation between the fracture aperture and the wellhead pressure in this artificial fracture was estimated by a transmissibility test (Hayashi and Abé, 1989). The fracture aperture was about 0.08mm without pressurization and 0.2mm at a wellhead pressure of 3.0MPa. The P-wave and S-wave velocities are about 2710m/s and 1730m/s, respectively (Sato *et al.*, 1986).

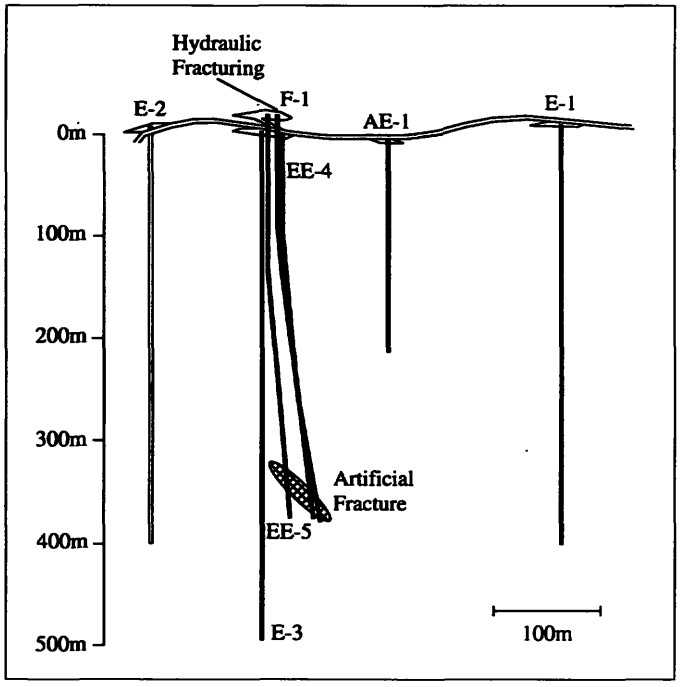

Figure 1. Higashi-Hachimantai Hot Dry Rock model field. EE-4 well and F-1 well intersects an artificial subsurface fracture at depths of 358.2m and 369.0m, respectively.

FWAL measurements were carried out in the depth range of 330-360m of well EE-4. A single receiver was deployed as a sonic tool with a 3ft source-receiver interval. The source center frequency is 15kHz. Wellheads of an injection well (Well F-1) and a production well (Well EE-4) were shut with wireline lubricators. Three FWAL logs were obtained maintaining well EE-4's wellhead pressure at 0MPa, 1MPa and 3MPa.

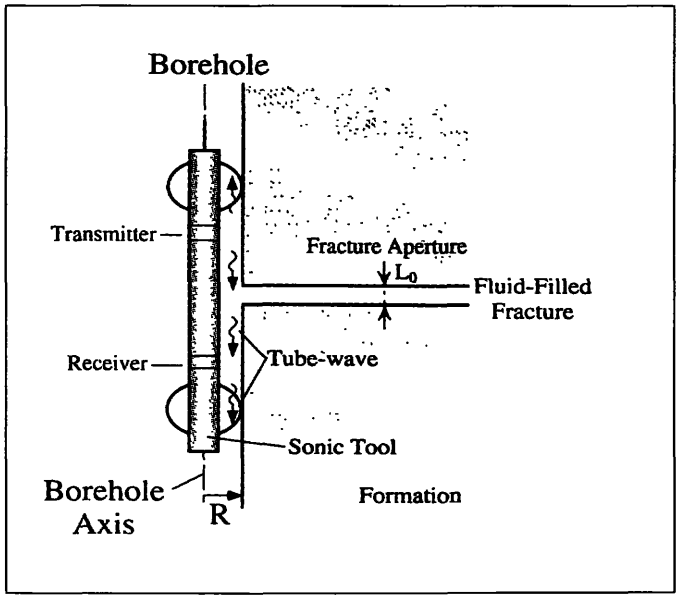

Figure 2. Diagram showing acoustic logging across an open borehole fracture.

Interpretive Model for Fracture Aperture

Next, we briefly outline the fracture aperture evaluation method. Figure 2 illustrates the configuration of borehole, a logging tool, the fracture and surrounding formations. The fracture is modeled as a plane-parallel channel of thickness L_0 and of infinite extent. When the Stoneley wave propagates across a fracture, interaction between the borehole fluid and the fracture occurs because of dynamic fluid conduction into the fracture; therefore the Stoneley wave attenuates and generates a reflected wave. The refraction and transmission coefficients of the Stoneley wave are given by following equations (Tang and Chen, 1989):

$$R_{ef} = -\frac{Y}{1+Y} \tag{1}$$

$$T_{rs} = \frac{1}{1+Y} \tag{2}$$

where

$$Y = \frac{\rho_0 c}{2} C\left[kn \frac{I_0(nR)}{I_1(nR)} \frac{H_1^{(1)}(kR)}{H_1^{(1)}(kR)} - k^2\right] \tag{3}$$

$$C = \frac{i L_0}{\omega \rho_0} \tag{4}$$

$$k^2 = \frac{\omega^2}{\alpha_f^2} \tag{5}$$

$$n^2 = \kappa^2\left(1 - \frac{c^2}{\alpha_f^2}\right) \tag{6}$$

$$\kappa = \frac{\omega}{c} \tag{7}$$

C is the dynamic conductivity; ρ_0 is the density of borehole fluid; c is the phase velocity of borehole Stoneley wave; a_f is the acoustic velocity of fluid; R is the borehole radius; k is the horizontal wave number of the guided wave in fracture; n is the horizontal wave number of the borehole Stoneley wave; k is the vertical wave number of the borehole Stoneley wave; I_0 and I_1 are the modified first kind Bessel functions of order zero and one; $H_0^{(1)}$ and $H_1^{(1)}$ are Hankel functions of order zero and one; and L_0 is the fracture aperture to be determined.

Result and Discussion

Variable density logs after direct arrivals were removed are shown in figure 3(a) and (b), for wellhead pressures of 0MPa and 3MPa, respectively. The depth range is 357-360m. Upgoing

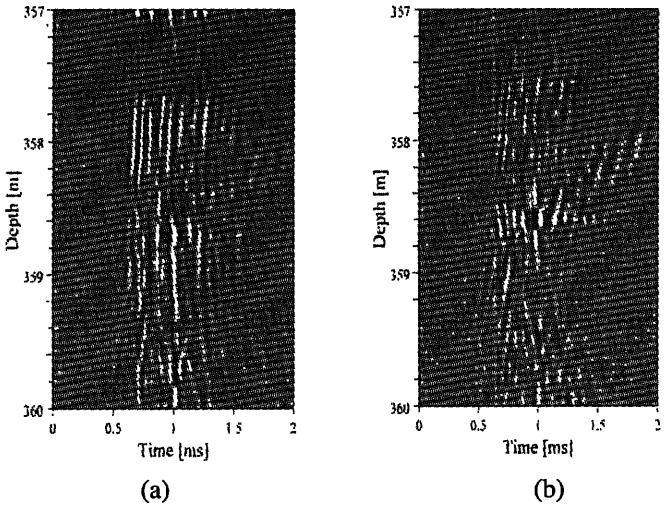

Figure 3. Variable density logs after direct arrivals were removed. The depth range is 357-360m. Upgoing and downgoing reflected tube waves are generated at the depth of around 359m. (a) The variable density log at a well EE-4's wellhead pressure of 0MPa. (b) The variable density log at a well EE-4's wellhead pressure of 3MPa.

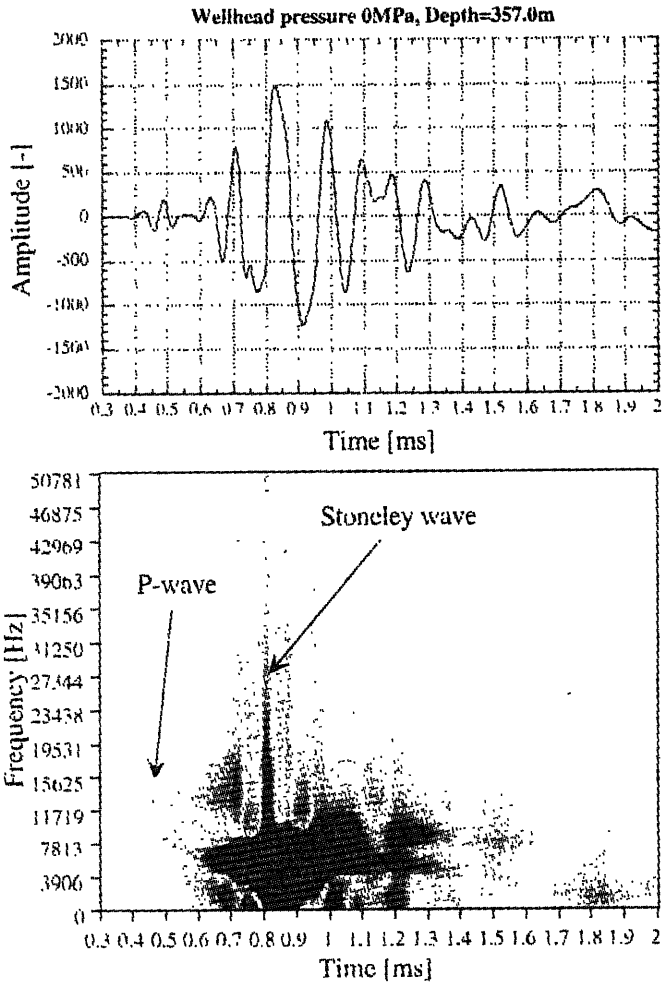

Figure 4. A typical waveform and an example of the time-frequency analysis. The waveform was recorded at the depth of 357m, at the wellhead pressure of 0MPa.

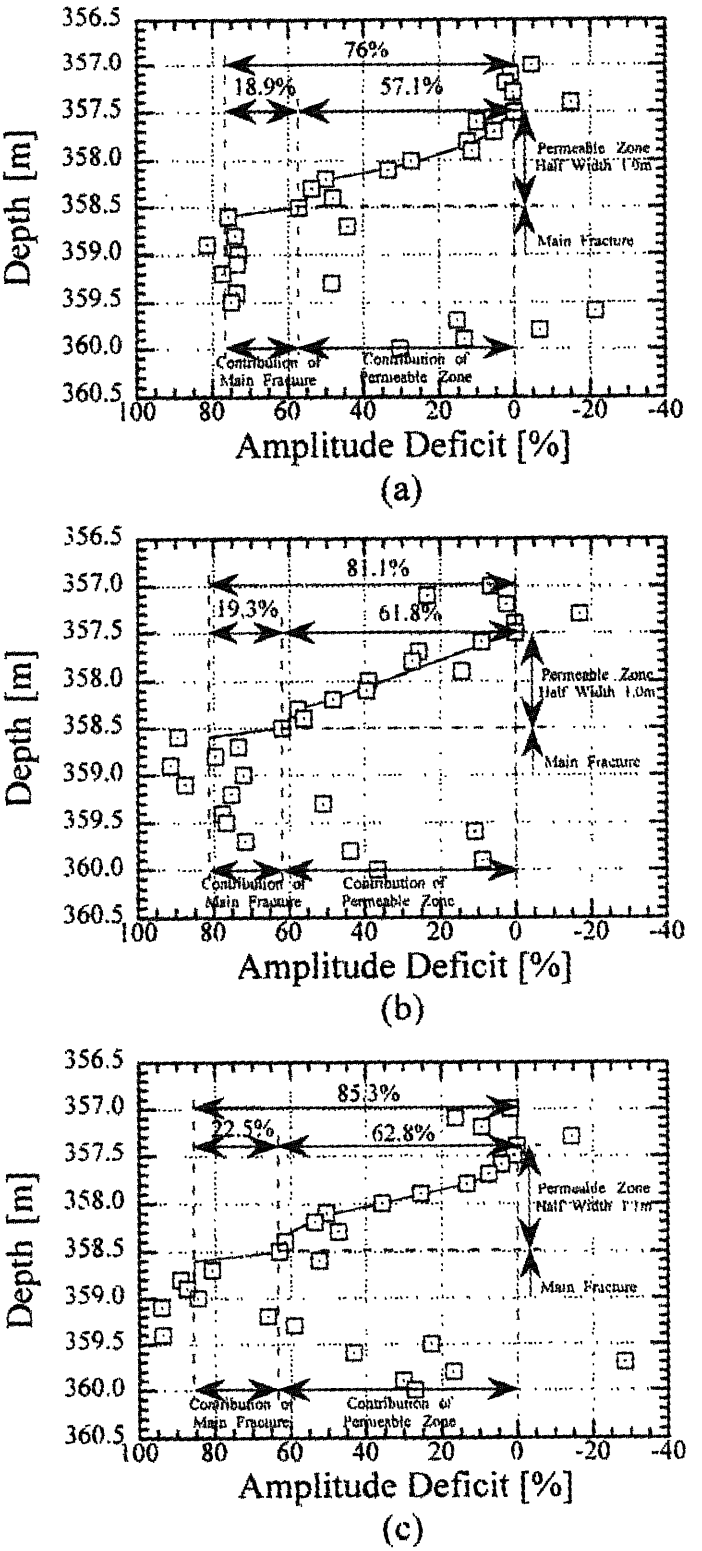

to pressurization is evident from this figure. (a) The amplitude deficit log at a well EE-4's wellhead pressure of 0MPa. (b) The amplitude deficit log at a well EE-4's wellhead pressure of 1MPa. (c) The amplitude deficit log at a well EE-4's wellhead pressure of 3MPa.

and downgoing reflected tube waves are generated at the depth of around 359m, as shown in figure 3(a), and as figure 3(b) shows more clearly. Therefore there is no doubt that the tube wave generation at the depth of around 359m is associated with the artificial fracture, and the increase of the fracture permeability due to pressurization is the main cause of increase of reflected tube wave amplitudes.

Waveform records were converted to amplitude logs by time-frequency analysis based on a Choi-Williams distribution (Moriya and Niitsuma, 1996). A typical waveform record and an example of the time-frequency analysis are shown in figure 4, where the darkness of the shading shows the magnitudes of the pressure oscillation. In the analysis, we observed P-wave amplitudes and transmitted tube-wave amplitudes in addition to the reflected tube-wave. Amplitude logs were then converted to amplitude deficit logs by integrating the difference between the local amplitude and the mean amplitude in adjacent unfractured intervals of borehole.

The P-wave amplitude deficit logs at wellhead pressures of 0MPa, 1MPa and 3MPa are shown in figure 5(a), (b) and (c), respectively. The maximum amplitude deficit increase and the range in which the amplitude deficits are observed widens slightly as wellhead pressure increases. One notable feature of the amplitude deficit logs is that the amplitude deficit increases at 357.5m, increases again from 358.5m and reaches its maximum at 358.6m depth. The most likely explanation of this feature is that the artificial fracture is embedded in a permeable zone. The thickness of the permeable zone is estimated as 1.4m considering the range of amplitude deficits and the dip of the fracture.

The transmitted Stoneley wave amplitude deficit logs are shown in figure 6(a), (b) and (c). The amplitude deficit increases and the range where the amplitude deficits are observed widens slightly as wellhead pressure increases. These features are similar to the P-wave. There is a difference in the pattern between the transmitted Stoneley wave amplitude deficit logs and the P-wave amplitude deficit logs, however. The difference is due to the differences of wavelength and raypath between the Stoneley wave and the P-wave.

Figure 7 shows the estimated aperture of the fracture based on transmission coefficient of the Stoneley wave as a function of wellhead pressure. The solid marks are calculated from equation (2). As Figure 7 indicates, the aperture of fracture widens as wellhead pressure increases.

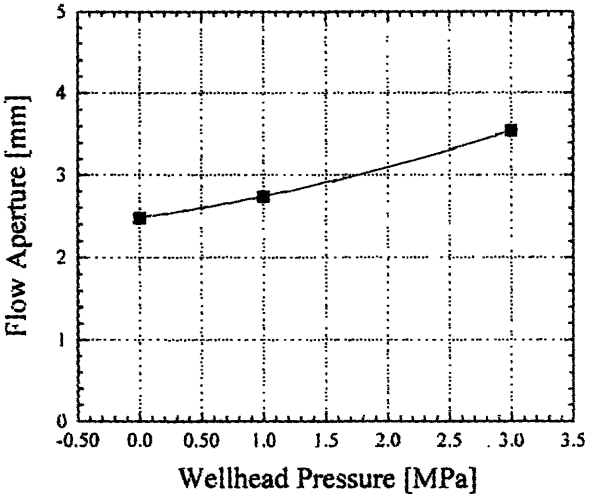

Figure 7. Estimated fracture aperture. The fracture aperture widens as wellhead pressure increase.

Table 1 (overleaf) shows physical parameters used in this study. The estimated fracture aperture and its change are about 20 times as large as obtained from the transmissibility test by Hayashi and Abé (1989). The major reason for the difference between the two methods is believed to be that the estimated aperture from the transmissibility test is averaged over the entire fracture zone, and that from FWAL data is only in the borehole vicinity. Table 2(overleaf) shows a summary of fracture characterization results obtained by P-wave and Stoneley wave amplitude deficit logs.

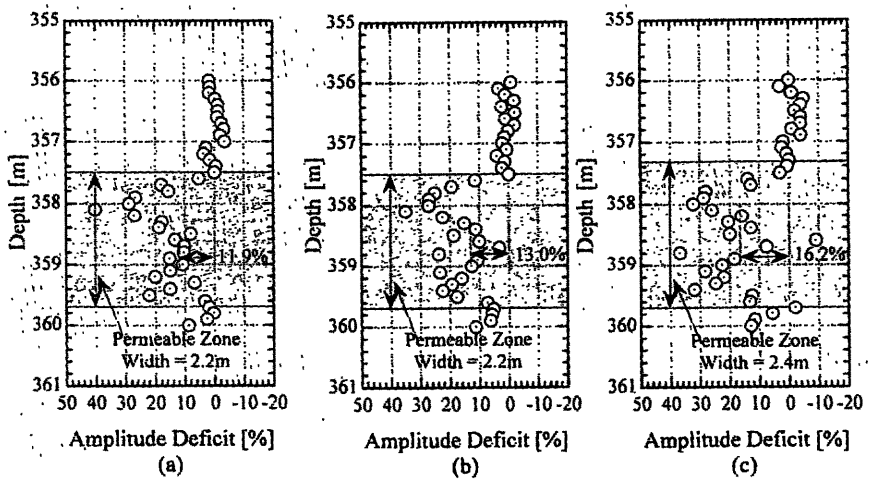

Figure 6. Amplitude deficit logs of transmitted Stoneley wave. Stoneley wave attenuation due to pressurization is evident from this figure. (a) The amplitude deficit log at a wellhead pressure of 0MPa. (b) The amplitude deficit log at a wellhead pressure of 1MPa. (c) The amplitude deficit log at a wellhead pressure of 3MPa.

Conclusion

In this study, we successfully detected changes of P-wave and Stoneley wave amplitudes propagating across the fracture, which depend on wellhead pressure. We have estimated fracture aperture and its change from transmitted tube-wave amplitude based on the theory of Tang and Cheng (1989). In addition, we have clarified the thickness of a permeable zone in the vicinity of the fracture. The conclusions that can be drawn from the present work are summarized as follows;

P-wave velocity (formation)	2710 (m/sec)
S-wave velocity (formation)	1730 (m/sec)
Density (formation)	2300 (kg/m^3)
Acoustic velocity (water)	1500 (m/sec)
Density (water)	1000 (kg/m^3)

Table 1. Physical parameters used in this study.

(1) The transmitted FWAL Stoneley wave analysis indicated that the estimated fracture aperture and its change were about 20 times as large as obtained from the transmissibility test.
(2) The amplitude deficit logs of the transmitted Stoneley wave and P-wave agreed that the thickness of permeable zone in the vicinity of the artificial fracture is about 1.4m.
(3) The increase in thickness of the permeable zone due to borehole pumping is no more than about 0.14m at a wellhead pressure of 3MPa.

(a) Results of P-wave

	Wellhead Pressure 0MPa	Wellhead Pressure 1MPa	Wellhead Pressure 3MPa
Half width of permeable zone	0.72m	0.72m	0.79m
Amplitude deficit at artificial fracture	76.0%	81.1%	85.3%

(b) Results of Stoneley wave

	Wellhead Pressure 0MPa	Wellhead Pressure 1MPa	Wellhead Pressure 3MPa
Width of permeable zone	1.58m	1.58m	1.73m
Amplitude deficit at artificial fracture	11.9%	13.0%	16.2%
Fracture aperture	2.48mm	2.74mm	3.55mm

Table 2. Summary of fracture characterization results obtained by P-wave and Stoneley wave amplitude deficit logs. (a) The result of P-wave. (b) The result of Stoneley wave.

Acknowledgement

This work was supported by the MURPHY/MTC project of the New Energy and Industrial Development of Japan and partly by the Ministry of Education, Science and Culture of Japan under the Grant-in-Aid for Scientific Research on Priority Areas (No. 03044023).

References

Hardin, E. L., C. H. Cheng, F. L. Paillet, and J. D. Mendelson, 1987, "Fracture characterization by means of attenuation and generation of tube waves in fractured crystalline rock at Mirror Lake, New Hampshire," *J. Geophys. Res.*, 92, 7989-8006.

Hayashi, K. and Abé, H., 1989, "Evaluation of Hydraulic Properties of the Artificial Subsurface System in Higashihachimantai Geothermal Model Field," *J. Geothermal Research Society of Japan*, 11, 203-215.

Mathieu, F., 1984, "Application of Full Waveform Acoustic Logging Data to the Estimation of Reservoir Permeability," *M.S. thesis, Mass. Inst. of Technol., Cambridge.*

Moriya, H and Niitsuma, H., 1995, "Detection of Micro Shear Wave Splitting in a Dilated Micro Crack Zone by Crosshole Three-Component Seismic Measurement," *Proc. 3rd SEGJ/SEG Int. Symp,* 55-62.

Moriya, H. and Niitsuma, H., 1996, "Precise Detection of a P-wave in Low S/N Signals by Using Time-Frequency Representation of a Triaxial Hodogram," *Geophysics,* 60, 1453-1466.

Niitsuma, H., 1989, "Fracture Mechanics Design and Development of HDR Reservoirs – Concept and Results of the G-project, Tohoku University, Japan," *Int. J. Rock Meck. Min. Sci. and Geomeck. Abstr.,* 26, 169-175.

Niitsuma, H. and Saito, H., 1991a, "Characterization of a Subsurface Artificial Fracture by the Triaxial Shear Shadow Method," *Geophys. J. Int.*, 107, 485-491.

Niitsuma, H. and Saito, H., 1991b, "Evaluation of the Three-Dimensional Configuration of a Subsurface Artificial Fracture by the Triaxial Shear Shadow Method," *Geophysics*, 56, 2118-2128.

Paillet, F. L., 1980, "Acoustic Propagation in the Vicinity of Fractures which Intersect a Fluid-filled Borehole," *Trans. SPWLA 21th Annu. Logging Symp.*, paper DD, 33p.

Sato, M., Nakatsuka, K., Niitsuma, H. and Yokoyama, H., 1986, "Calibration of Downhole AE Measurement System by Detonation Test," *Proc. of 8th. AE Symp. NDI, Japan*, 389-395.

Tang, X. M. and Cheng, C. H., 1989, "A Dynamic Model for Fluid Flow in Open Borehole Fractures," *J. Geophys. Res.*, 94, 7567-7576.